NASA TECHNICAL MEMORANDUM

NASA TM X-1812

NASA TM X-1812

THE FUEL-EMITTER SEPARATION PROBLEM IN EXTERNALLY FUELED THERMIONIC DIODES

by Harry W. Davison

Lewis Research Center

Cleveland, Ohio

NATIONAL AERONAUTICS AND SPACE ADMINISTRATION • WASHINGTON, D. C. • JUNE 1969

NASA TM X-1812

THE FUEL-EMITTER SEPARATION PROBLEM IN EXTERNALLY FUELED THERMIONIC DIODES

By Harry W. Davison

Lewis Research Center
Cleveland, Ohio

NATIONAL AERONAUTICS AND SPACE ADMINISTRATION

For sale by the Clearinghouse for Federal Scientific and Technical Information
Springfield, Virginia 22151 – CFSTI price $3.00

ABSTRACT

The fuel temperature and reactor power responses following fuel-emitter separation were calculated using a one-dimensional, linearized, time-dependent-heat-transfer model. The time-dependent power density in the fuel is calculated using space-independent, monoenergetic neutron diffusion theory. Six neutron delay groups and temperature coefficients of reactivity for all diode components are included in the analysis. Fuel melting is predicted in the reference diode design, and radial cooling fins are recommended as a design modification to avoiding fuel melting.

THE FUEL-EMITTER SEPARATION PROBLEM IN EXTERNALLY FUELED THERMIONIC DIODES

by Harry W. Davison

Lewis Research Center

SUMMARY

Several thermionic reactor concepts have been investigated for electric-power generation in space. One concept provides externally UO_2-fueled thermionic diodes which are cooled by liquid lithium flowing in a coaxial channel at the center of the diode. Because of the difference between the coefficients of thermal expansion for the fuel and emitter, temperature increases within the fuel might cause the fuel to "pull away" from the emitter. This situation might result in fuel melting and a subsequent nuclear catastrophy.

The consequences of fuel-emitter separation were analyzed mathematically by performing linearized transient heat transfer and neutronic calculations on a reference design externally fueled thermionic diode. The purpose of the study is to determine if fuel melting would occur and how long it might take to initiate fuel melting. The results of the study indicate that the problem is severe enough to cause fuel melting. If fuel-emitter separation occurs in all the diodes in the reactor, the power rise accompanying separation could be detected by neutron flux monitors and reactor power could be reduced in time to avoid fuel melting. If, however, fuel-emitter separation occurs in only a few diodes, reactor power changes will be too small to be detected by neutron flux monitors and melting of the fuel will occur until sufficient time elapses to allow the fuel to be vaporized and redeposited on the tungsten emitter.

One method of avoiding fuel melting involves placing radial tungsten fins in the fuel region to allow conduction of heat from the fuel, through the fin, and into the emitter. If eight 6-mil- (0.015 cm) wide fins are incorporated in the reference diode design, fuel melting could be avoided after fuel-emitter separation. The redesign would also require a 3 percent increase in reactor volume and a 1.7 percent increase in fuel outer radius in order to maintain reactor criticality.

INTRODUCTION

Many power-source concepts are currently being investigated for electric power generation in space. Several of these concepts combine thermionic diodes which convert thermal energy to electrical energy and a nuclear power source which provides thermal energy from the fission of nuclear fuel. One thermionic reactor design discussed in reference 1 incorporates a fueled-diode arrangement called an "externally fueled flashlight" configuration. In this design, the fuel assemblies are hollow cylinders which surround a diode configuration with a central, coaxial cooling passage as shown in figure 1. The UO_2 fuel surrounding the diode is the source of thermal power.

Ward and Ruch (ref. 2) recognized that the fuel will tend to separate from the diode when the temperature rises because the coefficient of thermal expansion of the fuel is higher than that of the diode emitter. If the fuel separates from the emitter, the resistance to heat conduction will increase and the fuel temperature will rise until the heat generated within the fuel can be transfered to the emitter. The temperature reached under these circumstances may be high enough to melt the fuel. Fuel melting must be avoided because it might result in damage to the clad due to rapid release of gaseous fission products; a greater loss of UO_2 fuel from fully vented fuel elements; a chemical reaction between the fuel and the clad causing a loss of clad strength; and a nuclear excursion caused by redistribution of the fuel.

The purpose of this study is to determine

(1) The fuel temperature response as a result of fuel-emitter separation

(2) How long it takes to initiate fuel melting (This information is required for the design of reactor safety circuits.)

(3) What design modifications might be made to the fuel assembly or in operating conditions either to prevent fuel-emitter separation or to prevent fuel melting.

The reference design of the thermionic fuel assembly is described first. This is followed by a description of the mechanisms associated with fuel-emitter separation. Calculated values of the temperature response following separation are described next and various methods of avoiding fuel melting are discussed.

SYMBOLS

A	area
C	reactivity coefficient
ΔC	thickness of fuel clad
C_p	heat capacity

F	mass flow rate
f_F	volume fraction of fuel in reactor
h	forced convection film coefficient
k	thermal conductivity
L	neutron lifetime
l	length of fuel cell
M	molecular weight
m	mass velocity of fuel vaporized
n	number of heat conducting fins
P	pressure
Q/A	heat flux
q	power density
R	specific radial field point
ΔR	spacing between fuel and emitter after accident
r	general radial field point
T	temperature
t	time
U	overall heat-transfer coefficient
V	volume
w	fin width
β	total delayed neutron fraction
ϵ	thermal emissivity
η	diode efficiency
Γ	reactivity
λ	decay constant
ρ	density
σ	Stefan-Boltzmann constant
θ	angle

Subscripts:

B	coolant
BE	end clad-to-emitter
BF	end clad-to-fuel
BP	end clad
b	boundary between fuel and cooling fin
C	collector
E	emitter
F	fuel
f	initial value
I	insulator
in	coolant inlet
max	maximum
o	coolant outlet
p	pipe
r	reactor core
s	surface

DESCRIPTION OF REFERENCE DESIGN THERMIONIC FUEL ASSEMBLY

A preliminary design of a fuel element containing externally fueled thermionic diodes was presented by Yacobucci (ref. 1) and a conceptual drawing of the fuel element is shown in figure 1. These fuel elements are uniformly distributed throughout a nuclear reactor and are electrically connected such that the desired electrical power output can be obtained. The diodes in each fuel element are stacked vertically along the length of the fuel element as illustrated in figure 1. The diodes are electrically connected in series and are physically separated by an electrical insulator. A typical diode contains a central coolant tube surrounded by the following concentric components:

(1) An Al_2O_3 electrical insulator which separates the collector from the coolant tube
(2) A niobium collector
(3) An interelectrode gap
(4) A tungsten emitter

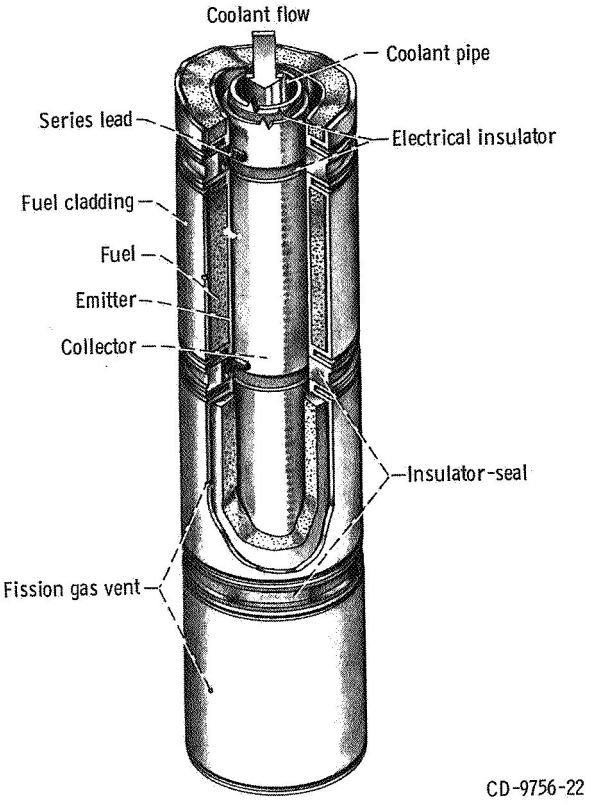

Figure 1. - Fuel element containing externally-fueled diodes.

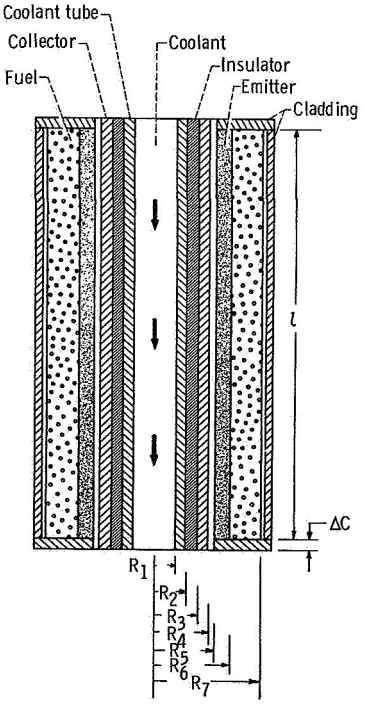

Figure 2. - Schematic drawing of externally fueled thermionic diode.

TABLE I. - NOMINAL CELL DIMENSIONS

[Cell length = 1 inch (2.54 cm).]

Component	Outer radius of component		Material
	in.	cm	
Coolant channel (R_1)	0.1605	0.4077	Li
Pipe (R_2)	.2005	.5093	Nb
Insulator (R_3)	.2105	.5347	Al_2O_3
Collector (R_4)	.2360	.5994	Nb
Interelectrode gap (R_5)	.2460	.6248	-----
Emitter (R_6)	.2660	.6756	W
Fuel (R_7)	.4290	1.090	UO_2
Clad (R_8)	.4490	1.140	W

TABLE II. - REACTOR OPERATING CONDITIONS

Thermal	
Power density, Btu/(sec)(ft^3); W/cm^3	3800; 142
Coolant flow, lbm/sec; kg/sec	0.079; 0.036
Emitter heat flux, Btu/(sec)(ft^2); W/cm^2	68; 77
Diode efficiency, percent	11
Nuclear	
Initial reactivity, $\Gamma(0)$	0.0
Neutron lifetime, sec	4.0×10^{-6}
β_1	0.22×10^{-3}
β_2	1.50×10^{-3}
β_3	1.33×10^{-3}
β_4	2.69×10^{-3}
β_5	0.78×10^{-3}
β_6	0.28×10^{-3}
β_{eff}	6.8×10^{-3}
λ_1, sec^{-1}	1.24×10^{-2}
λ_2, sec^{-1}	3.05×10^{-2}
λ_3, sec^{-1}	1.11×10^{-1}
λ_4, sec^{-1}	3.01×10^{-1}
λ_5, sec^{-1}	1.13
λ_6, sec^{-1}	3.0

(5) Uranium dioxide fuel

(6) Tungsten clad

The components and dimensional symbols of a typical diode are schematically illustrated in figure 2. The nominal diode dimensions used in the thermal analysis are presented in table I. Reactor operating conditions are summarized in table II, along with some neutron kinetic properties of the reference reactor.

DESCRIPTION OF FUEL-EMITTER SEPARATION MECHANISMS

The mechanisms associated with the fuel-emitter separation problem may be defined as

(1) The physical separation of the fuel from the emitter caused by some thermal perturbation in the fuel or emitter

(2) Subsequent impairment of heat transfer from the fuel causing the fuel temperature to increase and the emitter temperature to decrease

(3) Possible reactor power excursion caused by the reactivity addition associated with a reduction in emitter temperature (negative temperature coefficient of reactivity) or an increase in fuel temperature (positive temperature coefficient of reactivity)

Any perturbation in reactor power or coolant flow tending to increase the fuel temperature might cause the fuel to separate from the emitter because the coefficient of thermal expansion for the uranium dioxide fuel is about twice as large as that of the tungsten emitter. Therefore, the fuel expansion per degree temperature rise is greater than the emitter expansion and the fuel will tend to "pull away" from the emitter when the fuel temperature increases. The bond between the fuel and emitter may not be strong enough to keep the fuel from separating from the emitter. After separation, the resistance to heat transfer between the fuel and emitter will increase. The size of the gap between the fuel and emitter is presented in figure 3 as a function of the rise in the fuel and emitter temperature. The gap size was calculated with coefficients of thermal expansion of $6.74\times10^{-6}\ {}^{o}R^{-1}$ ($1.22\times10^{-5}\ K^{-1}$) and $3.16\times10^{-6}\ {}^{o}R^{-1}$ ($5.68\times10^{-6}\ K^{-1}$) for the fuel (ref. 3) and emitter (ref. 4), respectively.

The heat generated in the fuel can be dissipated by radiation to the emitter, mass transfer as a result of the fuel vaporizing and condensing on the cooler emitter, and conduction around the fuel-emitter gap through the end clad shown in figure 2. The fuel temperature will rise until the heat can be dissipated. The temperature rise may be sufficiently large to cause fuel melting. Fuel melting should be avoided because of the potential danger from rapid release of fission products and chemical reaction between the fuel and clad. Also, if a sufficient number of fuel assemblies melt, the redistribu-

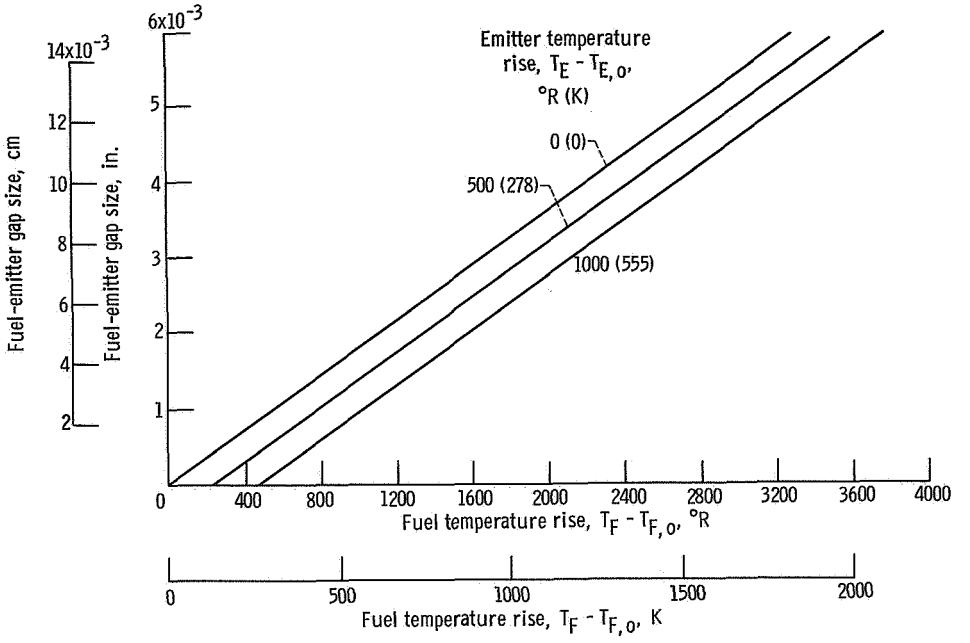

Figure 3. - Gap formed when fuel separates from emitter.

tion of fuel might introduce sufficient positive reactivity to cause a reactor power excursion and subsequent violent disassembly of the reactor structure.

If the fuel emitter separation occurs in only a few assemblies, no detectable change in reactor power will occur. If, however, separation occurs in many fuel assemblies, reactor power will be affected because of the temperature coefficient of reactivity associated with the fuel assembly components. If the reactivity of the reactor increases as a result of the temperature change, reactor power and fuel temperature will increase. Because of the potential effect of reactivity coefficients on reactor power and temperature, it is necessary to investigate the time-dependent neutronics response as well as the temperature response of the reactor.

TEMPERATURE RESPONSE AFTER SEPARATION

The temperature response of the fuel assembly components after fuel-emitter separation were calculated using the mathematical model described in appendix A. This model allows the calculation of the one-dimensional (radial), time-dependent temperatures of each of the major components of the diode. Axial heat loss from the fuel to the end clad is permitted. All modes of heat transfer are approximated as linear functions of temperature and no mass transfer between the fuel and emitter is permitted. The diode emitter current density is assumed to be constant after separation. This is a

valid assumption because the diodes are electrically connected in series and, therefore, all experience the same current. The time-dependent power density in the fuel is calculated using space-independent, monoenergetic, neutron kinetics equations. Six neutron delay groups are included and the effect of component temperature variations on reactivity (Doppler coefficients) are incorporated in the kinetics equation.

The temperature and power responses were calculated for three separate conditions:

(1) Fuel-emitter separation occurs in a single diode such that there is no appreciable change in reactor reactivity as the temperature of the diode components vary.

(2) Fuel-emitter separation occurs in all diodes in the reactor and reactor reactivity depends upon the temperature coefficients of reactivity and the temperature of the diode components. The temperature coefficients of reactivity for the reference design diode have not been calculated.

The temperature coefficients of reactivity shown in the following table are comparable to those used by other investigators (unpublished information obtained by C. R. Fisher, A. J. Gietzen, C. A. Heath, W. G. Homeyer, and D. R. Mathews of General Atomics) for their study of the unit cell thermionic reactor design.

Component	Reactivity coefficient	
	$/°R	$/K
Fuel	0	0
Emitter	-1.6×10^{-4}	-2.9×10^{-4}
Collector	-4.1×10^{-4}	-7.4×10^{-4}
Insulator	-5.3×10^{-5}	-9.5×10^{-5}
Pipe	-4.1×10^{-4}	-7.4×10^{-4}
Coolant	0	0

(3) Same as condition 2 except that the temperature coefficient of reactivity of the fuel is 8.0×10^{-5} \$/°R (1.4×10^{-4} \$/K).

The initial (before accident) component temperatures are summarized in table III. These temperatures were obtained from reference 1. The fuel-temperature rise, the emitter-temperature rise, and the relative reactor power are shown in figure 4 as a function of time after fuel-emitter separation. The reactor power is expressed relative to its initial value. The temperature changes in the coolant, coolant tube, insulator, and collector are much less than that of the fuel and emitter. Although these temperature changes were included in the calculations, they are generally too small to be illustrated in figure 4.

TABLE III. - INITIAL DIODE

TEMPERATURES

Temperature	°R	K
Maximum fuel	4860	2700
Emitter	3600	2000
Collector	2520	1400

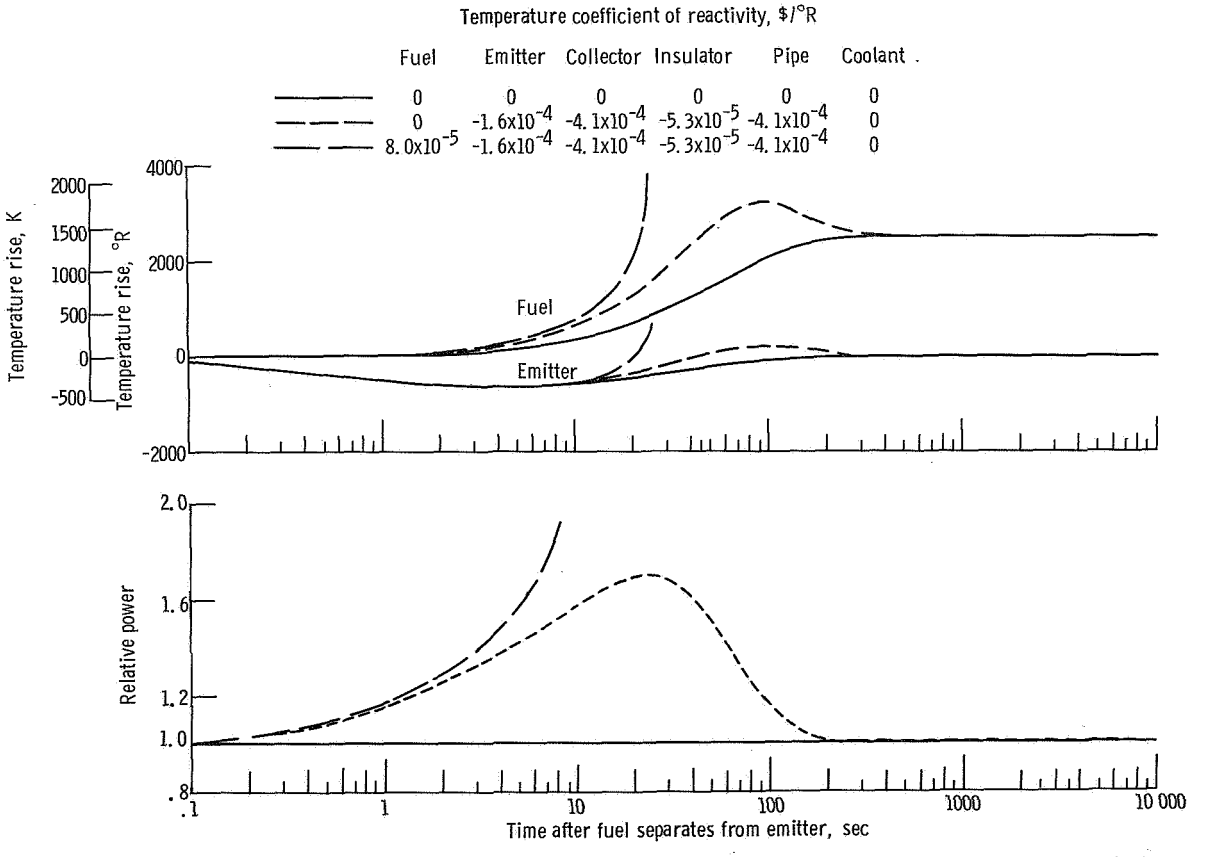

Figure 4. - Temperature and power response when fuel separates from emitter in an externally fueled thermionic diode.

Following fuel-emitter separation, a thermal resistance is introduced between the fuel and emitter. Therefore, the heat transfer to all components located inside the fuel is reduced and the temperature of these components decreases. This is illustrated in all three cases in figure 4 by the 600° to 700° R (330 to 390 K) reduction in emitter temperature which occurs within 5 seconds after the accident is initiated. During the same period, the fuel temperature rises because the resistance to heat removal from the fuel is increased when fuel-emitter separation occurs. Because there is no provision in the mathematical model for inclusion of the latent heat of fusion, melting cannot be accounted for.

The rates of change of fuel and emitter temperature and reactor power depend on the temperature coefficient of reactivity in the reactor.

(1) Case 1. When fuel-emitter separation occurs in a single diode, the fuel temperature rises about 200° R (111 K) in the first 5 seconds. At this time, the emitter temperature reaches a minimum value about 600° R (330 K) below its initial value. The fuel and emitter temperature continue to increase, thereafter, until equilibrium is reached about 300 seconds after separation. The final fuel temperature is about 2500° R (1390 K) higher than its initial value while the final emitter temperature is the same as its initial value. If, as is indicated in reference 1, the maximum initial fuel temperature is 4860° R (2700 K) and the UO_2 melting point is 5460° R (3030 K), the fuel will start to melt after the temperature has risen 600° R (330 K). From figure 4, the fuel would start to melt about 17 seconds after the fuel separates from the emitter. When the fuel separates from the emitter in a single diode there would be no detectable change in reactor power because the reactor reactivity change associated with fuel-emitter separation in a single diode is insignificant.

(2) Case 2. When fuel-emitter separation occurs in all the fuel cells but the temperature coefficient of reactivity in the fuel is zero, reactivity and power will increase as the emitter temperature decreases because of the negative temperature coefficient of reactivity associated with the emitter. After about 5 seconds, the emitter temperature reaches a minimum and starts to increase and reactor reactivity decreases. About 20 seconds after fuel-emitter separation the reactivity is too low to support a power rise, and reactor power decreases until it returns to the initial value about 300 seconds after separation. Both the fuel and emitter temperature reach maximum about 100 seconds after separation and decrease to equilibrium temperatures. The emitter equilibrium temperature is the same as the initial temperature and the fuel-equilibrium temperature is about 2500° R (1390 K) higher than the initial temperature. For the reference design, the fuel would start to melt about 9.5 seconds after separation.

(3) Case 3. The effect of a positive temperature coefficient of reactivity (8.0×10^{-5} $\$/^{\circ}R$) in the fuel was also investigated. In this case, the fuel temperature and power both rise faster than in the previous case because of the excess reactivity addition as-

sociated with the fuel temperature rise. For the reference reactor design conditions, the fuel would start to melt about 8 seconds after separation.

Fuel-emitter separation in all fuel cells would be accompanied by reactor power increases, as indicated in figure 4. Separation could probably be detected by neutron flux monitors and reactor power could be reduced before fuel melting occurred in the reactor. In case 2, a 20 percent increase in power would occur within 1.5 seconds leaving about 8.5 seconds to detect the abnormality and reduce power. Approximately 7 seconds warning time would be available in case 3.

It should be mentioned at this time that the 8.5- and 7-second warning times are based on an arbitrarily selected 20 percent power rise and depend upon the operating temperature of the fuel, fuel- and material-temperature coefficients of reactivity, and on the number of fuel cells which experience separation.

If the absolute values of the temperature coefficients of reactivity are smaller, or if only a few diodes experience fuel-emitter separation, the warning time would be reduced because the rate of power rise would be reduced. It would, therefore, take longer to detect a given power rise. When only a few cells experience fuel-emitter separation, it would be difficult to prevent fuel melting without monitoring the temperature of all fuel cells.

The calculated values of fuel temperature shown in figure 4 are conservative (high) because of several simplifying assumptions made in developing the mathematical model. Complete separation is assumed along the entire fuel-emitter interface. Actually some thermal contact would probably exist at some locations between the fuel and emitter after separation. Also, the thermal emissivities of the radiating surfaces were assumed to be equal (0.2) and independent of time. The mass transfer between the fuel and emitter surfaces was also neglected. Actually, the emissivity of the uranium dioxide is temperature dependent (therefore, it is time dependent) and a substantial fraction (about 20 percent is indicated in ref. 2) of the heat may be transferred across the fuel-emitter gap by mass transfer. This would reduce the thermal resistance between the fuel and emitter. The resulting change in fuel and emitter temperature and reactor power would be smaller. It would, therefore, take longer to detect a particular power change, but the fuel temperature change for a particular time after fuel-emitter separation would be less. The time-dependent effects of mass transfer have not been included in this study because the mass transfer cannot adequately be expressed as a linear function of temperature as required for solution by the AIROS (ref. 5) computer program. Estimates of the maximum fuel-temperature rise in a single fuel cell including both radiation and mass transfer indicate the fuel-temperature rise would still be greater than 1000° R (555 K) and the fuel would melt.

The high fuel temperatures would not persist indefinitely. After fuel-emitter separation the hot fuel would vaporize and redeposit on the cooler emitter surface reducing the maximum fuel temperature.

METHODS OF REDUCING FUEL TEMPERATURE

There are several potential methods of reducing the fuel temperature rise following fuel-emitter separation in an externally fueled diode. These include

(1) Use a heat-conducting gas annulus between the fuel and emitter

(2) Provide heat-conducting fins to transport the heat from the fuel to the emitter

(3) Alter the material in the fuel region to produce a negative temperature coefficient of reactivity

(4) Reduce the requirements on operating variables such as power density and coolant temperature

The first two methods will reduce the fuel temperature whether the separation occurs in only a few or many diodes. The third method will reduce the fuel temperature only when sufficient diodes are affected such that reactor power will be reduced. The last method either results in a larger reactor, reduced electric power output or both and is, therefore, the least attractive of the four methods. Only the first two methods were investigated in detail.

Gas Annulus

The fuel-emitter separation problem might be avoided by intentionally introducing a gap containing a heat-conducting inert gas (such as helium) between the fuel and emitter. A slightly higher design fuel temperature would be accepted in order to avoid the large fuel-temperature rise resulting after fuel-emitter separation. Thermodynamically, a heat-conduction resistance (the gas space) would be substituted for a thermal-radiation resistance. Therefore, for a given heat flux, the conduction across the helium gap would result in a smaller temperature difference between the fuel and emitter than would be expected with radiant heat transfer between the fuel and emitter.

The fuel-temperature rise resulting from variations in gap size would be about 130° R per mil (28 000 K/cm) increase in gap thickness if helium is used in the gap. During normal operation at 100 percent power in the reference system, an increase in gap size of about 5 mils (0.013 cm) could be tolerated without melting the fuel. Without the gas annulus, even less than 1-mil (0.003-cm) separation between the fuel and emitter would be sufficient to cause the fuel to melt. The increase in normal operating fuel temperature caused by introducing the gas annulus might be acceptable. If not, either the fuel thickness, power density, power distribution, or coolant temperature would have to be reduced to compensate for the excess temperature rise.

One potential problem associated with this method, however, is that the fuel might be vaporized, transferred across the helium annulus, and redeposited on the emitter. If

sufficient fuel is redeposited on the emitter, the redeposited fuel might again separate from the emitter if some perturbation in the system caused the fuel temperature to rise. The rate of UO_2 vaporized from the fuel surface was approximated using the relation presented in reference 6 for the evaporation of a material into a vacuum,

$$\dot{m} = 5.833\times10^{-2} P\sqrt{\frac{M}{T}}$$

where

$\dot{m}$ mass of UO_2 vaporized from fuel surface per unit time, $g/(cm^2)(sec)$

M gram molecular weight of material

P vapor pressure of material, mm Hg

T temperature, K

Using the procedure of Ward and Ruch (ref. 2), the net mass-transfer rate from the hot surface to the cooler surface is

$$\Delta\dot{m} = 5.833\times10^{-2}\left(\frac{P_H}{\sqrt{T_H}} - \frac{P_C}{\sqrt{T_C}}\right)\sqrt{M}$$

where the subscripts H and C refer to the hotter and cooler surfaces, respectively. The fuel vapor pressure P was approximated using the empirical correlation presented in reference 7

$$\log P = 13.340 - \frac{3.7337\times10^4}{T} + \frac{3.67\times10^6}{T^2} + \frac{2.4638\times10^9}{T^3}$$

where P is in millimeters of mercury and temperature T is in K.

The time required to transfer fuel across the helium gap is shown in figure 5 as a function of the relative thickness $(r - R_6)/(R_7 - R_6)$ of fuel transferred and helium gap width. Three modes of energy transfer were allowed in the calculation of the temperature rise across the helium gap; conduction, radiation, and mass transfer. The calculations are similar to those described in reference 2 except conduction is allowed across the helium. The results shown in figure 4 indicate that the fuel is transferred across the gap faster for large fuel-emitter gaps than for small gaps. This is expected because the larger gaps cause greater temperature differences across the gap and, thus, a

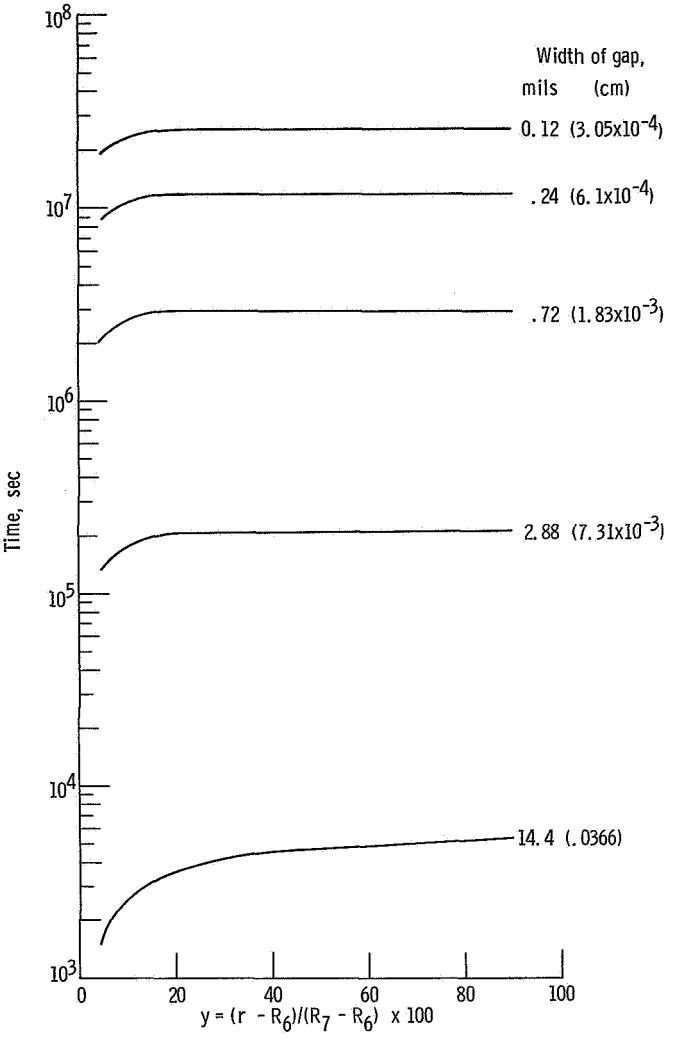

Figure 5. - Time required to transfer y percent of fuel thickness across helium gas gap.

greater driving force for mass transfer. However, even with a small 0.12 mil (3.05×10^{-4} cm) helium gap, 90 percent of the fuel would be redeposited on the emitter after about 7000 hours of reactor operation and the fuel would again be subject to melting caused by fuel-emitter separation if the helium does not migrate into the new fuel-emitter gap.

The presence of helium in the fuel-emitter gap may impede the vapor transport of UO_2 across the gap. Gluyas (ref. 8) showed that, at a particular temperature, the presence of argon at a pressure of 1 atmosphere could reduce the rate of mass transfer of UO_2 by an order of magnitude. However, since the rate of mass transfer of UO_2 across a helium gap is questionable, and because of the difficulty associated with maintaining any prescribed gap between the fuel and emitter during reactor operation, this method of avoiding fuel melting would probably have to be demonstrated.

Heat Conducting Fins

Another potential method of avoiding fuel melting is to provide fins which would conduct heat from the fuel to the emitter and, thus, reduce the maximum fuel temperature after the fuel separates from the emitter. A sketch of one possible finned thermionic diode concept is shown in figure 6. Radial-tungsten fins are incorporated within the fuel. The thermal conductivity of the tungsten is about 60 times better than that of the fuel. If fuel-emitter separation occurs, heat can be conducted from the fuel into the fin, and radially conducted along the fin into the tungsten emitter. Any thermal expansion induced in the fuel will tend to improve the contact between the fuel and the fin. The fuel and reactor diameters must be increased in order to add sufficient fuel to compensate for the additional fin material and to maintain nuclear criticality. The maximum temperature in the fuel was conservatively estimated by assuming only azimuthal heat conduction in the fuel, such that all of the heat generated in the fuel is radially transferred along the tungsten fin to the emitter. Reactor power and the emitter heat flux were assumed to be 208 kilowatts electric and 68 Btu per second per square foot, respectively (see pp. 40 and 41 of ref. 1). The reactor length was maintained at 18 inches (46 cm). Neutron and gamma heating in the tungsten fin is insignificant compared with the total heat generated in the fuel and was neglected. To simplify the mathematical analysis, the fin width was assumed to be proportional to the radius as shown in the sketch of a typical section of the fuel region shown in figure 7. The planes defined by $\theta = 0$ and $\theta = \theta_2$ are surfaces of symmetry, and the outer fuel surface is an adiabatic surface. Based upon these boundary conditions and assuming that the temperature of the fin root is equal

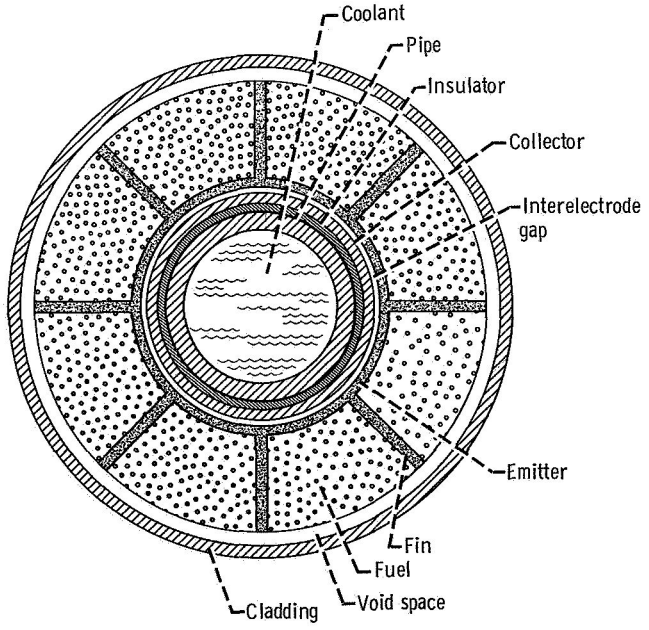

Figure 6. - Finned externally fueled diode.

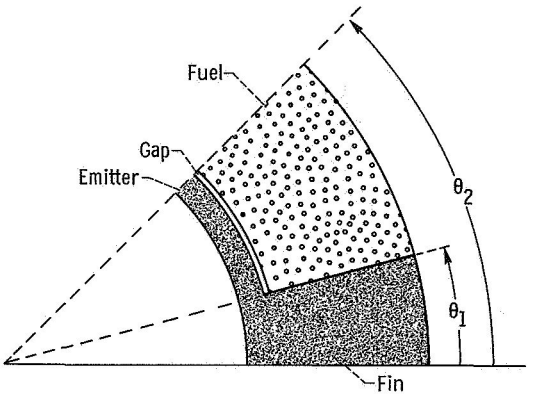

Figure 7. - Externally fueled thermionic diode with radial fin.

to the emitter temperature, the maximum fuel temperature can be approximated by the following equation which is derived in appendix B:

$$T_{F,\max} = T_E + \frac{q_F R_7^2 \left(1 - \frac{\theta_1}{\theta_2}\right)}{4k_F \frac{\theta_1}{\theta_2}} \left\{ \frac{2\pi^2 \frac{\theta_1}{\theta_2} \left(1 - \frac{\theta_1}{\theta_2}\right)}{n^2} + \frac{k_F}{k_E} \left[\frac{R_6^2}{R_7^2} - 1 + 2 \ln \left(\frac{R_7}{R_6} \right) \right] \right\}$$

With constant fuel and emitter thermal conductivities (k_F and k_E), the maximum fuel temperature depends on the volume fraction of fin in the fuel region θ_1/θ_2, the number of fins n, the fuel power density q_F, and the outer radius of the fuel R_7. The power density and fuel outer radius required to produce an emitter heat flux of 68 Btu per second per square foot (77 W/cm^2) and to maintain nuclear criticality depend upon the volume fraction of fin in the fuel. Therefore, q_F and R_2 were calculated for various volume fractions of fin in the fuel. The temperature difference ($T_{F,\max} - T_E$) is shown in figure 8 as a function of the volume fraction of fin in the fuel and the number of fins. As more fins are added, the maximum fuel temperature is reduced because the azimuthal heat conduction path in the fuel is reduced. As the volume fraction of fins in the fuel region is increased (each fin is made thicker), the fuel temperature is initially reduced because the heat transfer area of the fin is increased. However, the height of the fin must also be increased as the width is increased in order to add sufficient fuel to maintain reactor criticality. When the increase in fin height exceeds the increase in width, fuel temperature will have reached a minimum and will increase thereafter. The minimum fuel temperatures are obtained with fin volume fractions between 0.80 and 1.0.

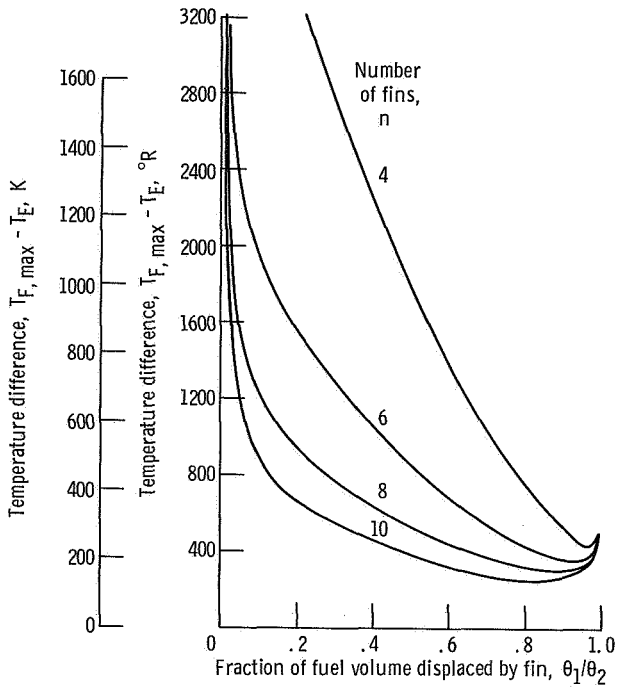

Figure 8. - Effect of fin design on maximum fuel temperature. Emitter heat flux, 77 watts per square centimeter (68 Btu/(sec)(ft^2)).

These results are shown in a different form in figure 9. The number of fins required to obtain various temperature rises is shown as a function of the volume fraction of fin in the fuel region. The relative volume of the reactor and the relative outer radius of the fuel required for criticality is also shown as a function of the volume fraction of fin in the fuel region. Although the lowest fuel temperatures would be obtained with fin volume fractions greater than 80 percent (fig. 8), the large increase in reactor size required for criticality would be impractical for space power considerations. In the reactor design of reference 1 the value of $T_{F,max} - T_E$ corresponding to fuel melting is 1860° R (1030 K). If fuel melting is to be avoided, the appropriate number of fins must be selected such that the temperature difference is less than 1860° R (1030 K). The number of fins must be selected such that a compromise is reached between final reactor volume and ease of fabricability of the fin. For example, four fins require a fin volume fraction θ_1/θ_2 of 0.48 in order to avoid fuel melting as shown in figure 8. However, as indicated in figure 9, the reactor volume would have to be increased by a factor of 2.5 to maintain criticality. The selection of 10 fins requires a fin volume fraction of 0.02. Although this requires a reactor volume increase of only 2 percent (from fig. 7), the fin root width w required with 10 fins (n = 10) and a volume fraction of 0.02 is

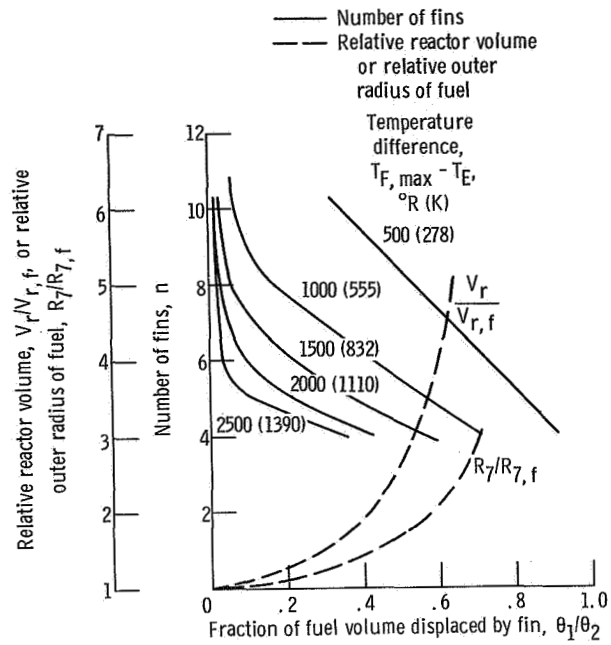

Figure 9. - Number of fins required and effect of fin size on reactor volume.

$$w = \frac{2\pi R_6 \frac{\theta_1}{\theta_2}}{n}$$

$$= \frac{2\pi\,(0.266)(0.02)}{10} = 0.0033 \text{ inch } (0.0084 \text{ cm})$$

It might be difficult to fabricate and assemble a fueled diode having a tungsten fin 3.3 mils (0.0084 cm) wide, 0.5 inch (1.27 cm) high and about 1 inch (2.54 cm) long.

For the reference design externally fueled thermionic diode, eight fins having a fin volume fraction of 0.03 and a fin root width of 0.006 inch (0.0152 cm) would keep the maximum fuel temperature below the melting point. The reactor volume and fuel outer radius would have to be increased by only about 3 percent and 1.7 percent, respectively, to maintain criticality.

CONCLUSIONS

The temperature response following separation of the fuel from the emitter in an externally fueled thermionic diode was calculated neglecting the mass transfer across

the fuel-emitter gap. The results of the study on the reference design externally fueled thermionic diode indicate

1. If fuel-emitter separation occurs in many diodes, the fuel would start to melt within about 8 to 10 seconds after separation if reactor power is not reduced. The power rise associated with this accident is sufficiently large to be detected by neutron flux monitors and could allow reactor power to be reduced before the fuel melts.

2. If, however, fuel-emitter separation occurs in only a few diodes, the fuel in these diodes could melt about 17 seconds after separation and there would be no detectable increase in neutron flux. Unless the temperature of the fuel material in each diode is monitored, there may be no way of detecting separation in time to prevent fuel melting.

Neglecting the effect of mass transfer across the fuel-emitter gap results in conservative (too high) fuel temperatures. However, steady-state calculations, including both the effects of mass transfer and radiation, indicate that the maximum fuel temperature would be less but fuel melting would still occur. The reduction in thermal resistance caused by the inclusion of mass transfer would also result in slower response times for fuel and emitter temperature and reactor power.

Several methods of reducing the fuel temperature rise after separation were investigated. The most attractive method required the redesign of the diode to include radial tungsten cooling fins in the fuel region which would allow conduction of heat from the fuel through the fin and into the emitter. It is desirable to minimize total fin volume because, to maintain nuclear criticality, reactor volume must be increased to compensate for the addition of fins. Therefore, a compromise must be reached between reactor volume and fabrication capability. For the reference design thermionic diode, fuel melting could be avoided by inserting eight fins in a diode. The required fin width is about 6 mils (0.015 cm). The reactor volume and fuel outer radius would have to be increased about 3 percent and 1.7 percent, respectively.

Lewis Research Center,
National Aeronautics and Space Administration,
Cleveland, Ohio, February 8, 1969,
120-27-05-20-22.

APPENDIX A

MATHEMATICAL MODEL

The time-dependent temperature distribution in the externally fueled thermionic diode was calculated using the digital computer program AIROS (ref. 5). This program allows the solution of simultaneous linear differential equations of first order and first degree. These equations are coupled to the space-independent reactor neutronics equation. The heat transfer through the diode was approximated using a one-dimensional (radial), time-dependent model. The model allows heat conduction through all components of the diode. Heat is removed by forced convection to an incompressible liquid coolant flowing through the coolant tube. Radiation between the fuel and clad after separation is approximated by a linear function of the temperature difference between the fuel and clad. The diode efficiency η is assumed constant throughout the transient.

The following equations represent a heat balance over each major diode component:

Coolant:

$$\rho_B C_{p_B} V_B \frac{dT_B}{dt} = U_p A_p (T_p - T_B) - 2F_B C_{p_B} (T_B - T_{in}) \tag{A1}$$

Coolant tube:

$$\rho_p C_{p_p} V_p \frac{dT_p}{dt} = U_I A_I (T_I - T_p) - U_p A_p (T_p - T_B) \tag{A2}$$

Insulator:

$$\rho_I C_{p_I} V_I \frac{dT_I}{dt} = U_C A_C (T_C - T_I) - U_I A_I (T_I - T_p) \tag{A3}$$

Collector:

$$\rho_C C_{p_C} V_C \frac{dT_C}{dt} = (1 - \eta) U_E A_E (T_E - T_C) - U_C A_C (T_C - T_I) \tag{A4}$$

Emitter:

$$\rho_E C_{p_E} V_E \frac{dT_E}{dt} = U_F A_F (T_{F,s} - T_E) - U_E A_E (T_E - T_C) + U_{BE} A_{BE} (T_{BP} - T_E) \tag{A5}$$

Fuel:

$$\rho_F C_{p_F} V_F \frac{dT_F}{dt} = q_F V_F - U_F A_F (T_{F,s} - T_E) - U_{BF} A_{BF} (T_F - T_{BP}) \tag{A6}$$

Unless otherwise indicated, the overall conductances $U_i A_i$, which are constant were calculated for initial, steady-state conditions. The bulk coolant temperature T_B is

$$T_B = \frac{T_{in} + T_o}{2} \tag{A7}$$

All component temperatures except the fuel surface temperature $T_{F,s}$ are taken at the radial midpoint of the component. The overall conductances used to describe the heat transfer between the pipe and coolant $U_p A_p$, insulator and pipe $U_I A_I$, and collector and insulator $U_C A_C$ are

$$U_p A_p = \frac{2\pi l}{\frac{1}{R_1 h} + \frac{\ln\left(\frac{R_1 + R_2}{2R_1}\right)}{k_p}} \tag{A8}$$

$$U_I A_I = \frac{2\pi l}{\frac{\ln\left(\frac{2R_2}{R_1 + R_2}\right)}{k_p} + \frac{\ln\left(\frac{R_2 + R_3}{2R_2}\right)}{k_I}} \tag{A9}$$

$$U_C A_C = \frac{2\pi l}{\frac{\ln\left(\frac{R_3 + R_4}{2R_3}\right)}{k_C} + \frac{\ln\left(\frac{2R_3}{R_2 + R_3}\right)}{k_I}} \tag{A10}$$

The overall conductance between the emitter and collector includes several modes of heat transfer. This conductance was obtained from a typical diode performance curve (ref. 1) by empirically expressing the heat flux as a function of temperature drop across the interelectrode gap for constant emitter current density. This relation is presented

in figure 10. If the accident occurred in a single cell, the current density would nearly be constant because all cells in a thermionic fuel assembly are connected in series. The empirical correlation for the overall conductance is

$$U_E A_E = 0.20229 - 1.2186\times10^{-4} (T_E - T_C) \tag{A11}$$

where $U_E A_E$ is in units of watts per ^{o}K, and T_E and T_C are in units of ^{o}K. Using initial values of T_E (2000 K) and T_C (1400 K),

$$U_E A_E = 0.244 \frac{\text{Btu}}{(\text{hr})(^{o}\text{R})} \left(0.129 \frac{\text{W}}{^{o}\text{K}}\right)$$

The overall conductance between the fuel and emitter after separation includes only radiant heat transfer and is expressed as

$$U_F A_F = \frac{2\pi\sigma l(R_6 + \Delta R)\left(T_{F,s}^3 + T_{F,s}^2 T_E + T_{F,s} T_E^2 + T_E^3\right)}{\frac{1}{\epsilon_F} + \left(\frac{R_6 + \Delta R}{R_6}\right)\left(\frac{1}{\epsilon_E} - 1\right)} \tag{A12}$$

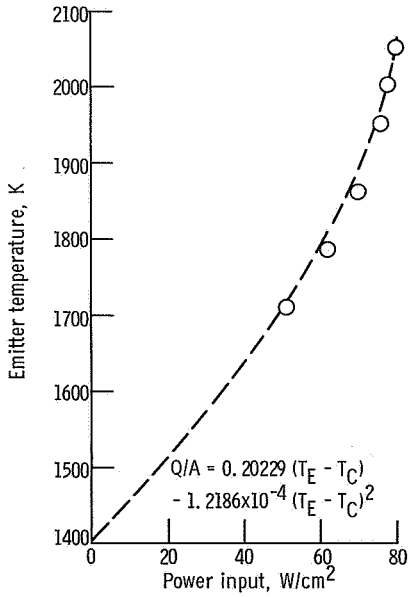

Figure 10. - Effect of input power on emitter temperature. Collector temperature, 2520° R (1400 K).

The final steady-state values of $T_{F,s}$ and T_E obtained using the initial fuel power density q_F were used to calculate $U_F A_F$. Prior to separation, the fuel and emitter are in thermal contact and $T_{F,s} \approx T_E$. The thermal driving force in equations (A5) and (A6) is $T_F - T_E$ instead of $T_{F,s} - T_E$ and

$$U_F A_F = \frac{2\pi l}{\frac{\ln\left(\frac{2R_6}{R_5 + R_6}\right)}{k_E} + \frac{2R_7^2 \ln\left(\frac{R_6 + R_7}{2R_6}\right) + R_6^2 - \left(\frac{R_6 + R_7}{2}\right)^2}{2k_F\left(R_7^2 - R_6^2\right)}} \tag{A13}$$

The difference between the fuel temperature T_F and the fuel-surface temperature $T_{F,s}$ is assumed to be independent of time.

Heat conduction from the fuel, through the end clad, and into the emitter is accounted for by the terms $U_{BE}A_{BE}(T_{BP} - T_E)$ and $U_{BF}A_{BF}(T_F - T_{BP})$ in equations (A5) and (A6).

$$U_{BE}A_{BE} = \frac{2\pi}{\frac{\ln\left(\frac{2R_6 + \Delta R}{R_6 + R_5}\right)}{k_{BP}\Delta C} + \frac{l}{k_E\left(R_6^2 - R_5^2\right)}} \tag{A14}$$

$$U_{BF}A_{BF} = \frac{2\pi}{\frac{\ln\left(\frac{R_6 + R_7 + 2\Delta R}{2R_6 + \Delta R}\right)}{k_{BP}\Delta C} + \frac{l}{k_F\left(R_7^2 - R_6^2\right)}} \tag{A15}$$

The temperature response of the end clad is calculated by

$$\rho_{BP}C_{p_{BP}}V_{BP}\frac{dT_{BP}}{dt} = U_{BF}A_{BF}(T_F - T_{BP}) - U_{BE}A_{BE}(T_{BP} - T_E) \tag{A16}$$

The reactor power and fuel assembly power density q_F were approximated by the monoenergetic space-independent neutronics equation including six delayed neutron groups:

$$\frac{dq_F}{dt} = \frac{\beta}{L}\left\{[\Gamma(t) - 1]\, q_F + \frac{L}{\beta}\sum_{i=1}^{6} \lambda_i q_{Di}(t)\right\} \tag{A17}$$

$$\frac{dq_{Di}}{dt} = \frac{\beta_i}{L} q_F - \lambda_i q_{Di} \tag{A18}$$

$$\beta = \sum_{i=1}^{6} \beta_i \tag{A19}$$

The effect of changes in the component temperatures on reactivity $\Gamma(t)$ is approximated using temperature coefficients of reactivity for each of the j components as follows

$$\Gamma(t) = \Gamma(0) + \sum_j C_j \left[T_j(t) - T_j(0)\right] \tag{A20}$$

where the reactivity Γ is in dollars.

Equations (A1) to (A19) are solved on a digital computer to determine the component temperature and power response as a function of time.

Calculations were performed using the cell dimensions presented in table I, fuel element operating conditions given in table II, initial temperatures shown in table III, and component property values shown in table IV.

TABLE IV. - COMPONENT PROPERTIES

Component	Material	Property	Value	Reference
Coolant	Li	ρ, lb/ft^3; g/cm^3	26.2; 0.420	9
		C_p, Btu/(lb)(^{O}R); J/(kg)(K)	0.996; 4169	9
		k, Btu/(sec)(ft)(^{O}R); W/(cm)(K)	1.04×10^{-2}; 0.648	9
Coolant tube	Nb	ρ, lb/ft^3; g/cm^3	535; 8.57	10
		C_p, Btu/(lb)(^{O}R); J/(kg)(K)	0.085; 355	10
		k, Btu/(sec)(ft)(^{O}R); W/(cm)(K)	9.7×10^{-3}; 0.61	10
Insulator	Al_2O_3	ρ, lb/ft^3; g/cm^3	240; 3.85	11
		C_p, Btu/(lb)(^{O}R); J/(kg)(K)	0.306; 1280	11
		k, Btu/(sec)(ft)(^{O}R); W/(cm)(K)	9.7×10^{-4}; 0.056	11
Collector	Nb	ρ, lb/ft^3; g/cm^3	535; 8.57	10
		C_p, Btu/(lb)(^{O}R); J/(kg)(K)	0.085; 355	10
		k, Btu/(sec)(ft)(^{O}R); W/(cm)(K)	9.7×10^{-3}; 0.61	10
Emitter	W	ρ, lb/ft^3; g/cm^3	1210; 19.4	4
		C_p, Btu/(lb)(^{O}R); J/(kg)(K)	0.035; 150	4
		k, Btu/(sec)(ft)(^{O}R); W/(cm)(K)	1.78×10^{-2}; 1.11	4
Fuel	UO_2	ρ, lb/ft^3; g/cm^3	684; 11.0	3
		C_p, Btu/(lb)(^{O}R); J/(kg)(K)	0.08; 300	3
		k, Btu/(sec)(ft)(^{O}R); W/(cm)(K)	2.78×10^{-4}; 0.0174	3
Clad	W	ρ, lb/ft^3; g/cm^3	1210; 19.4	4
		C_p, Btu/(lb)(^{O}R); J/(kg)(K)	0.035; 150	4
		k, Btu/(sec)(ft)(^{O}R); W/(cm)(K)	1.78×10^{-2}; 1.11	4

APPENDIX B

ESTIMATED HEAT TRANSFER FROM EXTERNALLY FUELED THERMIONIC DIODE CONTAINING RADIAL FINS

The temperature distribution in an externally fueled diode containing radial-cooling fins connecting the fuel with the emitter was estimated assuming only azimuthal heat conduction in the fuel and only radial heat conduction in the fin. Using the sketch shown in figure 7, the temperature distribution in the fuel region can be conservatively estimated if radial and axial heat transfer are neglected after fuel-emitter separation occurs. The Fourier equation is used to approximate the azimuthal heat conduction in the fuel having a fission (power) density of q_F:

$$\frac{1}{r^2}\frac{d^2T}{d\theta^2} = -\frac{q_F}{k_F}$$

If θ_2 is taken as the plane of symmetry between adjacent fuel regions and the temperature at the fuel-fin interface is T_B, the boundary conditions are

$$\frac{dT}{d\theta} = 0 \text{ at } \theta = \theta_2$$

$$T = T_B \text{ at } \theta = \theta_1$$

The azimuthal temperature distribution is:

$$T = T_B + \frac{q_F r^2}{2k_F}\left[\theta(2\theta_2 - \theta) - \theta_1(2\theta_2 - \theta_1)\right]$$

The steady-state heat transfer in the fin can be approximated with a heat balance over an incremental radius of fin, dr; that is, the heat transferred into the fin per unit length of the fuel is equal to the heat conducted radially out of the fin per unit length of fin:

$$rq_F(\theta_2 - \theta_1)\,dr = -k_E\frac{d}{dr}\left(\theta_1 r\frac{dT}{dr}\right)dr$$

Reduced to the simplest algebraic form, this equation becomes

$$\frac{d}{dr}\left(r\frac{dT}{dr}\right) = -\frac{q_F}{k_E}\left(\frac{\theta_2}{\theta_1} - 1\right)r$$

If no heat transfer is assumed from the outer radius of the fin R_7 and the temperature at the fin root R_6 is assumed to be the same as the emitter temperature, the boundary conditions for the fin are

$$\frac{dT}{dr} = 0 \quad \text{at} \quad r = R_7$$

$$T = T_E \quad \text{at} \quad r = R_6$$

The solution to the fin heat transfer equation is

$$T = T_E - \frac{q_F}{4k_E}\left(\frac{\theta_2}{\theta_1} - 1\right)\left[\left(r^2 - R_6^2\right) - 2R_7^2 \ln\left(\frac{r}{R_6}\right)\right]$$

The maximum temperature difference between fuel and emitter is

$$T_{F,\max} - T_E = \frac{q_F}{4k_E}\left(\frac{\theta_2}{\theta_1} - 1\right)\left[\left(R_6^2 - R_7^2\right) + 2R_7^2 \ln\left(\frac{R_7}{R_6}\right)\right] + \frac{q_F R_7^2}{2k_F}\left(\theta_2 - \theta_1\right)^2$$

or

$$T_{F,\max} - T_E = \frac{q_F R_7^2\left(1 - \frac{\theta_1}{\theta_2}\right)}{4k_F \frac{\theta_1}{\theta_2}}\left\{\frac{k_F}{k_E}\left[\frac{R_6^2}{R_7^2} - 1 + 2\ln\left(\frac{R_7}{R_6}\right)\right] + \frac{2\frac{\theta_1}{\theta_2}\left(1 - \frac{\theta_1}{\theta_2}\right)}{\frac{1}{\theta_2^2}}\right\}$$

The number of fins in a diode n is equal to the circumference of the fuel $2\pi r$ times the fin volume fraction θ_1/θ_2 divided by the width of each fin $2\theta_1 r$:

$$n = \frac{2\pi r \frac{\theta_1}{\theta_2}}{2\theta_1 r}$$

or

$$n = \frac{\pi}{\theta_2}$$

The maximum temperature rise across fuel and fins can be expressed in terms of the fuel volumetric heating rate q_F, material thermal conductivity ratio k_F/k_E, fuel dimensions R_6 and R_7, fin volume fraction θ_1/θ_2, and number of fins connecting the fuel with emitter n:

$$T_{F,\max} - T_E = \frac{q_F R_7^2 \left(1 - \frac{\theta_1}{\theta_2}\right)}{4k_F \left(\frac{\theta_1}{\theta_2}\right)} \left\{ \frac{2\pi^2 \frac{\theta_1}{\theta_2} \left(1 - \frac{\theta_1}{\theta_2}\right)}{n^2} + \frac{k_F}{k_E} \left[\frac{R_6^2}{R_7^2} - 1 + 2 \ln \left(\frac{R_7}{R_6} \right) \right] \right\}$$

REFERENCES

1. Yacobucci, Howard G.: Preliminary Study of a Thermionic Reactor Core Composed of Short-Length Externally Fueled Diodes. NASA TN D-4805, 1968.

2. Ward, James J; and Ruch, Robert B.: Uranium Dioxide Vent Loss in an Externally Fueled Thermionic Reactor Concept. NASA TN D-4922, 1968.

3. Burdi, G. F.: SNAP Technology Handbook. Vol. III, Refractory Fuels and Claddings. NAA-SR-8617, Atomics International, 1964.

4. Goldsmith, Alexander; Waterman, Thomas E.; and Hirschorn, Harry J.: Thermophysical Properties of Solid Materials. Vol. I - Elements (Melting Temperature Above 1000° F). Armour Research Foundation (WADD-TR-58-476, vol. 1), Aug. 1960.

5. Blaine, R. A.; and Berland, R. F.: AIROS - A Digital Simulator For Power Reactor Dynamics. Rep. NAA-SR-9943, Atomics International, Aug. 1, 1964.

6. Dushman, Saul: Scientific Foundations of Vacuum Technique. Second ed., John Wiley & Sons, Inc., 1962.

7. Ackermann, Raymond J.: The High Temperature, High Vacuum Vaporization and Thermodynamic Properties of Uranium Dioxide. Rep. ANL-5482, Argonne National Lab., Sept. 14, 1955.

8. Gluyas, Richard E.: Calculation of Fuel Loss from Vented Nuclear Fuel Elements for Space Power Reactors. NASA TN D-4913, 1968.

9. Davison, Harry W.: Compilation of Thermophysical Properties of Liquid Lithium. NASA TN D-4650, 1968.

10. Bartlett, E. S.; and Houch, J. A.: Physical and Mechanical Properties of Columbium and Columbium-Base Alloys. DMIC 125, Batelle Memorial Inst., Feb. 22, 1960.

11. Touloukian, Y. S., ed.: Recommended Values of the Thermophysical Properties of Eight Alloys, Major Constituents and Their Oxides. Purdue Univ., Feb. 1966.

NASA-Langley, 1969 —— 22 E-4935

NATIONAL AERONAUTICS AND SPACE ADMINISTRATION
WASHINGTON, D.C. 20546

OFFICIAL BUSINESS

FIRST CLASS MAIL

POSTAGE AND FEES PAID
NATIONAL AERONAUTICS AND
SPACE ADMINISTRATION

POSTMASTER: If Undeliverable (Section 158
Postal Manual) Do Not Return

"The aeronautical and space activities of the United States shall be conducted so as to contribute . . . to the expansion of human knowledge of phenomena in the atmosphere and space. The Administration shall provide for the widest practicable and appropriate dissemination of information concerning its activities and the results thereof."

—NATIONAL AERONAUTICS AND SPACE ACT OF 1958

NASA SCIENTIFIC AND TECHNICAL PUBLICATIONS

TECHNICAL REPORTS: Scientific and technical information considered important, complete, and a lasting contribution to existing knowledge.

TECHNICAL NOTES: Information less broad in scope but nevertheless of importance as a contribution to existing knowledge.

TECHNICAL MEMORANDUMS: Information receiving limited distribution because of preliminary data, security classification, or other reasons.

CONTRACTOR REPORTS: Scientific and technical information generated under a NASA contract or grant and considered an important contribution to existing knowledge.

TECHNICAL TRANSLATIONS: Information published in a foreign language considered to merit NASA distribution in English.

SPECIAL PUBLICATIONS: Information derived from or of value to NASA activities. Publications include conference proceedings, monographs, data compilations, handbooks, sourcebooks, and special bibliographies.

TECHNOLOGY UTILIZATION PUBLICATIONS: Information on technology used by NASA that may be of particular interest in commercial and other non-aerospace applications. Publications include Tech Briefs, Technology Utilization Reports and Notes, and Technology Surveys.

Details on the availability of these publications may be obtained from:

SCIENTIFIC AND TECHNICAL INFORMATION DIVISION

NATIONAL AERONAUTICS AND SPACE ADMINISTRATION

Washington, D.C. 20546